Preparation and Characterization of Double-Layered Microencapsulated Red Phosphorus and Its Flame Retardance in Poly(lactic acid)

Shaokun Chang,[1] Chao Zeng,[1] Weizhong Yuan,[1] Jie Ren[1,2]

[1]*Institute of Nano and Bio-Polymeric Materials, Tongji University, Shanghai, China*
[2]*Key Laboratory of Advanced Civil Engineering Materials, Ministry of Education, Tongji University, Shanghai, China*

Received 21 December 2010; accepted 5 November 2011
DOI 10.1002/app.36449
Published online 1 February 2012 in Wiley Online Library (wileyonlinelibrary.com).

ABSTRACT: A novel double-layered microencapsulated red phosphorus (DMRP) has been prepared through chemical precipitation of aluminum trihydrate (ATH) and *in situ* polymerization of melamine formaldehyde (MF) resin on the red phosphorus (RP) powder surface, and its structure was characterized by Fourier transform infrared (FTIR) spectroscopy and scanning electron microscopy (SEM). The influence of DMRP on flame retardance and thermal stability of poly(lactic acid) (PLA) was thoroughly investigated by means of X-ray diffractometry (XRD), limiting oxygen index (LOI), vertical burning test, and thermogravimetric analysis (TGA). With an optimum mass ratio of RP/ATH/MF = 72.25%/12.75%/15%, it has been found that PLA with the addition of DMRP at 25 wt % loading level shows good flame retardance compared to plain RP as well as the conventional microencapsulated red phosphorus (CMRP), and can achieve UL94 V-0 rating along with an LOI increase from 20.5 to 29.3. The TGA and XRD studies indicate that the interaction occurs among all three components: RP, ATH, and MF resin. © 2012 Wiley Periodicals, Inc. J Appl Polym Sci 125: 3014–3022, 2012

Key words: microencapsulation; flame retardance; biodegradable; poly(lactic acid)

INTRODUCTION

Because of the disposal difficulty of nondegradable petroleum-based plastics, nowadays, biodegradable polymeric material has continuously received increasing attention as it can fundamentally alleviate the white contamination.[1] Poly(lactic acid) is one of the biodegradable polymers that has been widely studied for use in biomedical applications because of its bioresorbable and biocompatible properties.[2–4] It can be synthesized by direct condensation polymerization of lactic acid or by ring opening polymerization of lactide and can be efficiently derived from renewable resources such as sugarcane, potato, and other nongrain agricultural products. Moreover, with good mechanical strength, thermal plasticity, high modulus, high degree of transparency, and ease of fabrication, PLA has also got a large momentum for various applications in agriculture, packaging, electronic and electric industry, automobiles, and so on.[5–10]

Though burning with a clean blue flame without generating any poisonous or corrosive gases, the large-scale application and further development of PLA in some important fields have been restricted because of its poor fire-resistance. Hitherto some research work has been done. Fontaine et al.[11] studied the intumescent polylactide and found that the combination of melamine and ammonium polyphosphate (APP) at 10 wt % loading showed a 30% reduction of the peak of the rate of heat released (pRHR) as compared to plain PLA, and could achieve UL94 V-0. But APP is easy to migrate due to poor compatibility with polymer matrix and tends to hydrolyze when exposed in a moist environment.[12] Zhan et al.[13] synthesized an intumescent flame retardant spirocyclic pentaerythritol bisphosphorate disphosphoryl melamine (SPDPM). It is found that the composites reached UL94 V-0 and the LOI value was increased to 38 at 25 wt % loading. Yamashita et al.[14] focused on the effects of metal oxides on the thermal degradation behavior of poly(lactic acid) and found that the flammability properties of PLA were modified and a shift to lower temperature in TGA curves was observed. However, all of these flame retardants (FR) have certain disadvantages. Either heavy loadings are generally needed to reach a suitable flame-retardant level, or a large amount of organic solvent should be used unavoidably during the synthesis process, thus may lead to some undesirable changes in physical and mechanical properties of the composites as well as environmental concern.

In recent years, with the development of halogen-free flame retardants worldwide, red phosphorus has been widely applied in many polymers due to

Correspondence to: J. Ren (renjie6598@163.com).

its high phosphorus content, low cost, and low toxicity. Nevertheless, red phosphorus is an unstable substance and undergoes a disproportionation reaction with moisture and oxygen to decompose and thus generate phosphine, which is harmful to human body. As a result, some special surface treatments are needed to modify the properties of RP when used as a flame retardant. The conventional methods involve inorganic and organic microencapsulation.[15,16] However, the conventional microencapsulated RP which is encapsulated with a single layer still has a tendency to react with moisture. Furthermore, inorganically encapsulated RP shows an easily damage of encapsulation layer, relatively low ignition point, and poor compatibility with polymers.

In our previous work, the flame retardation and thermal degradation of PLA/montmorillonite and PLA/APP series have been studied.[17–19] The aim of the present work is to investigate the flammability properties of flame-retarded PLA composites containing double-layered microencapsulated RP. Aluminum sulfate (AS) and MF resin were selected here to conduct such a coating treatment.

EXPERIMENTAL

Materials

The PLA (2002D, specific gravity = 1.24, melt index = 5–7 g/10 min) is a commercial product of NatureWorks, USA. It is a clear extrusion sheet grade and can be processed easily on conventional extrusion and thermoforming equipments. RP is a granulated product supplied by Shanghai Xusen Non-halogen Smoke Suppressing Fire Retardants, China. AS, melamine, formaldehyde, and sodium dodecyl sulfate (SDS) were purchased from Sinopharm Chemical Reagent, China. All these commercial chemicals were used as received without further purification.

Preparation of double-layered microencapsulated RP

Synthesis of MF prepolymer

Melamine and 37 wt % formaldehyde solution were put into a three-necked bottle with a mole ratio of 1 : 3. The mixture was heated to 70°C under continuous magnetic stirring and the pH was adjusted to 8–9 with 25 wt % ammonia solution. Approximately 1 h later, the colorless transparent MF prepolymer solution was prepared.

Chemical precipitation of ATH and *in situ* polymerization of MF prepolymer

The granulated RP (50 g) and proper amount of 5 wt % sulfuric acid solution (500 mL) were added into a three-necked bottle equipped with a reflux condenser. The mixture was heated to 100°C under continuous magnetic stirring and kept at that temperature refluxing for 2 h. The suspension was then filtered, washed twice with distilled water, and refluxed for 2 h with proper amount of 5 wt % NaOH solution (500 mL). After filtered, washed again and dried, the pretreated RP was finally obtained. These procedures are expected to remove the metal impurities such as Fe and Cu, which could further result in the instability of red phosphorus. The pretreated RP (5 g), 1.0% SDS (0.05 g, calculated from the amount of RP), proper amount of distilled water (50 mL) and calculated amount of 10 wt % AS solution were then mixed in a three-necked bottle and heated to 70°C. After predispersing for 10 min, the pH of the suspension was adjusted to 8–9 to conduct the chemical precipitation reaction of Al^{3+}, through which ATH was expected to be deposited on the surface of RP particle. Approximately 2 h later, calculated amount of MF prepolymer solution was added into the suspension and the pH was adjusted to 4–5 to conduct the *in situ* polymerization. The resulting mixture was incubated at the same temperature for 2 h. The suspension was then filtered, washed twice, dried, and pulverized to a fine powder with a particle size of about 120 meshes. Thus the DMRP was finally obtained, while the CMRP could also be prepared by this procedure without conducting the MF prepolymer synthesis and *in situ* polymerization.

Preparation of flame-retarded PLA composites

PLA pellets were dried at 80°C under vacuum for 6 h before used. All flame-retarded PLA composites were prepared in a two-roll mixing mill (SK-160B, Shanghai, China) for 20 min with a temperature of about 165°C and a roll speed of 35 rpm. After milling, the samples were first hot-pressed at 170°C under 20 MPa for 5 min and then cold-pressed at room temperature under 10 MPa for 2 min into sheets of 3 mm thickness for characterization.

Characterization

The moisture absorption rate of RP products was measured by putting 2 g of sample in a culture dish (10 cm), which was then placed into a constant temperature and constant humidity box (GDS-225, China) for 48 h with a setting temperature and humidity, 65°C and 95%, respectively. The increasing weight percentage of the sample was finally calculated. The ignition point was carefully observed and recorded by putting 1 g of sample into a ceramic crucible, which was then placed into an electric heating furnace with a heating rate of 2°C min^{-1}. Particle

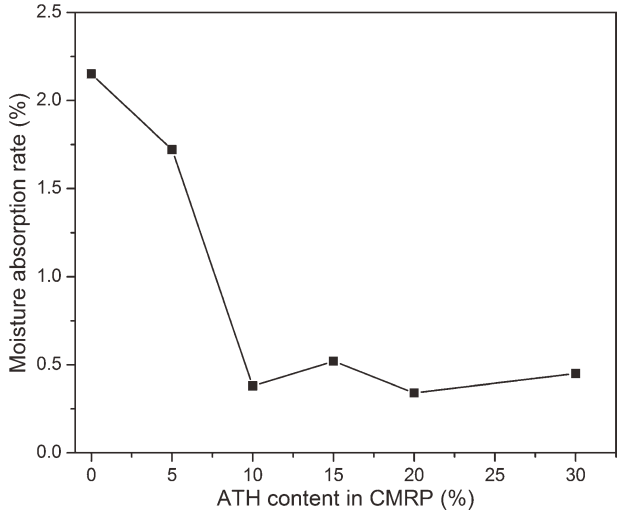

Figure 1 Moisture absorption rates of CMRP with different ATH content.

size distribution was measured by laser particle size analyzer (LS230, Beckman Coulter, USA). All of the suspensions awaiting particle size analysis were directly sampled from the preparation process of microencapsulated RP to improve the reliability of experimental data. The FTIR spectra were recorded with a Bruker EQUINOXSS/HYPERION2000 spectrometer using KBr pellet. The morphology of the samples was observed by SEM Quanta 200 FEG (FEI Company). LOI values were measured by a HC-2 oxygen index meter (Jiangning Analysis Instrument Company, China) according to ASTM D2863. The specimens used for the test were of dimensions of $100 \times 6.5 \times 3$ mm^3. UL94 vertical burning test was carried out on a CFZ-2-type instrument (Jiangning Analysis Instrument Company, China) according to ASTM D3801 UL94 standard with the specimen dimensions of $125 \times 13 \times 3$ mm^3. To study the structure of the carbonaceous residue, X-ray diffractometer (D/max2550VB3+/PC, Rigaku International Corporation, USA) was utilized with a pretreatment of the sample by maintaining it at 500°C for 2 h to eliminate the organic part. TGA was performed both in air flow and nitrogen flow (30 mL min^{-1}) on a Pyris 1 apparatus (PERKIN ELMER, USA) at a heating rate of 20°C min^{-1}. The weight of all samples were kept within 3–5 mg in an open TGA pan and heated from ambient temperature to 700°C.

RESULTS AND DISCUSSION

Moisture absorption rate and ignition point

Red phosphorus can react with moisture and oxygen and thus generate metaphosphoric acid, phosphoric acid, polyphosphoric acid, and poisonous phosphine. Furthermore, the decomposition products adversely affect properties of the flame-retarded resin and corrode the mold in molding the resin. As a result, it is essential to restrict the contacting area between RP and moist air. Figure 1 shows the moisture absorption rate evolution of CMRP versus ATH content. It can be clearly observed that the moisture absorption rate of pretreated RP was as high as 2.15%, however, was only 0.45% when 30 wt % ATH (calculated from the amount of CMRP) was added, and it had the tendency to decrease as the ATH content increased, which could be attributed to a more thickened and complete microcapsule.

ATH is selected here as an inorganic layer. Such a filler is preferable because it serves to improve the mechanical strength of the resinous coating layer to be polymerized on the CMRP particle surface as well as its flame-retardant efficiency and produce the effect of hiding the purplish red color characteristic of RP to thereby contribute to the expansion of the application of RP flame retardants. Moreover, several flame retardation mechanisms may be involved such as action on PLA viscosity in the molten state, catalytic action on degradation products promoting char formation, and oxidation of red phosphorus or phosphorus compounds.[20]

The ignition point of pretreated RP is 248°C (Fig. 2), but it is significantly increased to 257°C after only 5 wt % ATH was incorporated. When the ATH content was increased to 10, 15, 20, and 30 wt %, the ignition point is continuously elevated to 282, 299, 311, and 323°C, respectively. Haurie et al.[21] reported that the thermal decomposition of aluminum trihydrate was a strong endothermic step between 190 and 350°C with a mass loss of 35%. It indicates its low decomposition temperature, which could effectively decrease the temperature in the surroundings of the material as it involves huge amount of heat absorption (about 280 calories per gram ATH), thus the

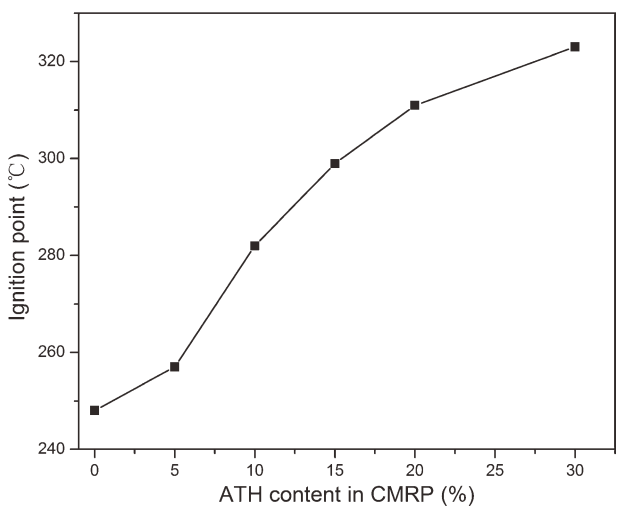

Figure 2 Ignition points of CMRP with different ATH content.

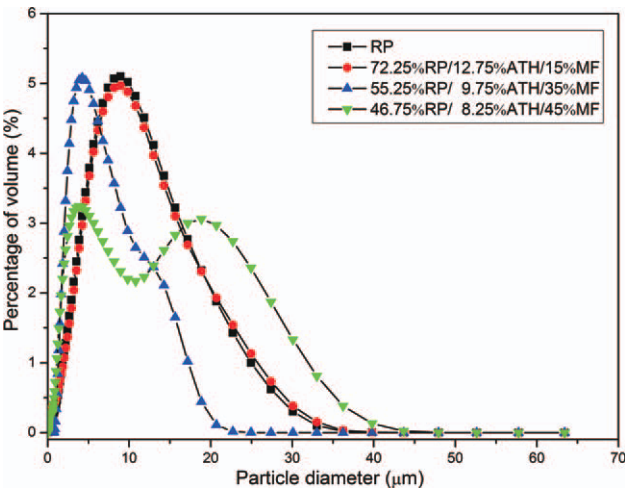

Figure 3 Particle size distributions of RP and DMRP with different formulation. [Color figure can be viewed in the online issue, which is available at wileyonlinelibrary.com.]

ignition point of CMRP was increased. In addition, the decomposition process of ATH is well matched with the thermal degradation of PLA. Kopinke et al.[22] have pointed out that the PLA decomposes with two well-resolved endothermic peaks ranging from 225°C to about 370°C. In this range, ATH will decompose efficiently and it may also be possible that the trihydrate could take part in a chemical reaction with RP, which we will focus on later in this article. Its chemically combined water is then released into the gas phase. This dilutes the flammable gases around the burning substrate and also hinders it from further access to atmospheric oxygen. Hence, $Al(OH)_3$ will act as a heat sink fin in PLA and produce water vapor and thus reduce its flammability. Nevertheless, it is not true that the performance of the composites will be better with increasing amount of ATH in CMRP, because a side effect is the deterioration of mechanical strength of the composites as well as dispersity of the flame retardant.

Particle size analysis

Figure 3 illustrates that MF content has a significant influence on the mean size and size distribution of the encapsulated samples. The four distributions have a similar spread (from 0.04 μm to about 64 μm) in the particle size. The volume mean diameter of pretreated RP is ~ 8.777 μm whereas for DMRP, they are 8.715, 5.799, and 8.996 μm at 15 wt % ATH level (calculated from the amount of CMRP) with the corresponding MF content 15% (calculated from the amount of DMRP), 35 wt % and 45 wt %, respectively (Table I). By increasing the MF content at a low level, the particle size distribution shifts slightly to the left indicating a decrease in the mean particle size. A similar phenomenon has been observed by Wu et al.[23] This is because the surfactant SDS and the thermosetting resin reduce the aggregation of microcapsules. However, a distortion occurred when MF content is as high as 35 wt %, and a bimodal distribution at 45 wt %. A possible reason is that the excess MF prepolymer polymerized and cured in the aqueous suspension instead of depositing on the RP particle surface. The difference of the volume characteristic between RP and MF resin particle has resulted in the bimodal distribution and a broader particle size distribution span with a value of 3.87 when 45 wt % MF resin was incorporated.

To form a fine dispersion as well as good flame retardance in polymer composites, a small particle size and a narrow particle size distribution of flame retardants are generally needed.[24] Therefore, the MF resin content should be restricted.

Spectroscopic analysis

Because of the relatively high moisture absorption rate, the FTIR spectrum of pretreated RP [Fig. 4(a)] shows two distinct water vapor absorption peaks at 3430 and 1637 cm^{-1}. The reaction products of RP with water vapor include metaphosphoric acid and phosphoric acid, thus a broad absorption band at about 1184 cm^{-1} (P=O, stretching vibration) is generated. However, no significant difference has been observed between CMRP [Fig. 4(b)] and pretreated RP. For DMRP [Fig. 4(c)], the main absorption peaks appear at 3397, 1562, 1494, 1340, 1153, and 811 cm^{-1}. The peak at 3397 cm^{-1} is corresponding to the stretching vibration of N-H. The absorptions of 1562, 1494, 1340 and 811 cm^{-1} are due to the ring vibration of melamine. The 1138 cm^{-1} band is representative of

TABLE I
Results of Particle Size Analysis

Sample	Mean particle size (μm)	Size distribution span	Cumulative volume				
			10% (μm)	25% (μm)	50% (μm)	75% (μm)	90% (μm)
RP	8.777	2.06	1.897	4.182	7.559	12.08	17.45
72.25%RP/12.75%ATH/15%MF	8.715	2.19	1.437	3.965	7.445	12.06	17.74
55.25%RP/ 9.75%ATH/35%MF	5.799	2.17	1.872	2.859	4.634	7.690	11.93
46.75%RP/ 8.25%ATH/45%MF	8.996	3.87	1.335	2.597	5.461	13.79	22.48

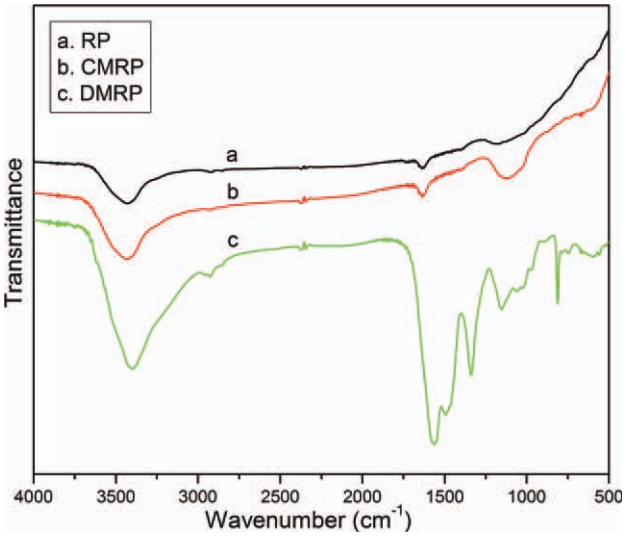

Figure 4 FTIR spectra of (a) RP, (b) CMRP, (c) DMRP (CMRP: RP/ATH = 85%/15%, DMRP: RP/ATH/MF = 72.25%/12.75%/15%).[Color figure can be viewed in the online issue, which is available at wileyonlinelibrary.com.]

symmetric C—O—C of —CH_2—O—CH_2— between melamine groups. Based on the analysis, the DMRP spectrum reveals only the well-defined absorption peaks of MF resin without any characteristic bands of RP. This indicates that RP particles are well encapsulated.

Morphology

To give an intuitive description of the surface structure of RP products, all samples were analyzed by SEM and depicted in Figure 5. Pretreated RP consists of relatively big aggregates [Fig. 5(a)], which can be attributed to the reaction between RP and H_2O. It leads to the formation of viscous compounds that easily connects RP particles together. In addition, since the pulverizing step is indispensable during the production process, the contour of each RP particle is constituted by split-off surface having many active sites. They are so reactive that the disproportionation reaction and the generation of

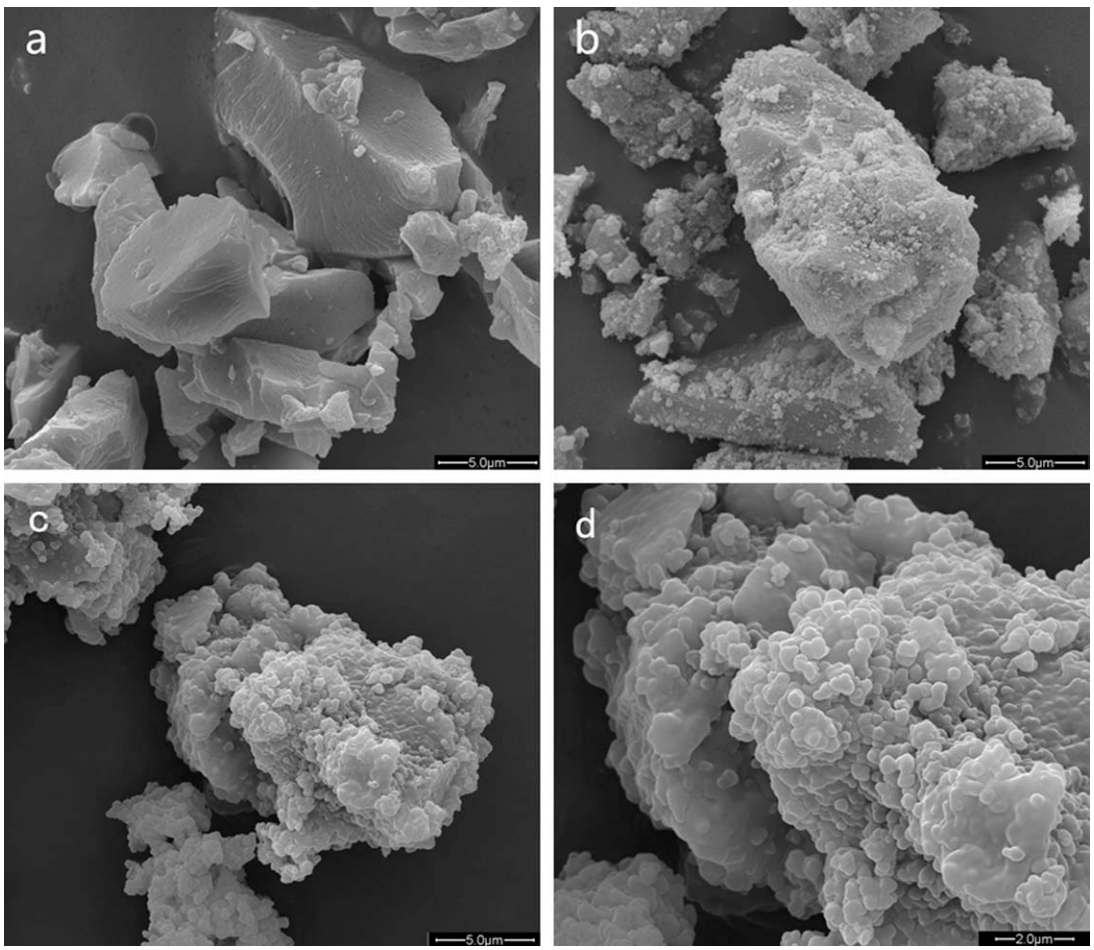

Figure 5 SEM micrographs of (a) RP (×10,000), (b) CMRP (×10,000), (c) DMRP (×10,000), (d) DMRP (×20,000) (CMRP: RP/ATH = 85%/15%, DMRP: RP/ATH/MF = 72.25%/12.75%/15%).

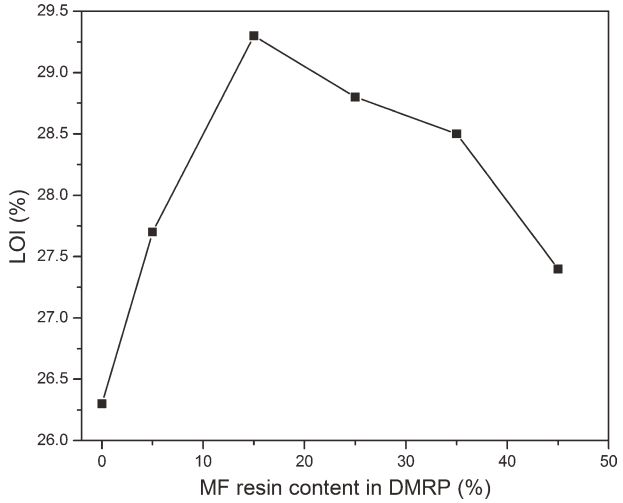

Figure 6 LOI values of PLA-DMRP blends with different MF resin content (at 25 wt % FR loading).

harmful substances are much accelerated. However, in Figure 5(b), the situation has been improved because the chemically stable inorganic component is well deposited on the particle. The original split-off surfaces are refinished to become a sphere or ellipsoid like shape, and a core-shell structure with RP as a core and ATH as a shell is formed, which could effectively protect the active sites inside. Besides, the incorporation of SDS as well as the decrease of moisture absorption rate also results in the reduction of agglomeration of microcapsules as compared to pretreated RP. The morphology of DMRP is presented in Figure 5(c). It can be seen that the CMRP particles are fully enwrapped. During the dispersion step, RP particles coated with ATH will diffuse into the MF prepolymer network. And due to the addition of SDS and magnetic stirring, this process is expected to proceed successfully. Then, the relatively low pH catalyzes polycondensation of MF prepolymer and promotes the formation of a pyknotic cross-linked structure that covers on CMRP.

Combustion performance

PLA is selected here as a matrix resin to evaluate the flame retardance of double-layered microencapsulated red phosphorus. First, the relationship between flame retardance and the MF resin content in DMRP (with a constant mass ratio of RP/ATH = 85%/15%) was investigated. At 25 wt % loading level, the LOI of CMRP flame-retarded PLA is only 26.3 (Fig. 6). However, the LOI value varies significantly as the resin content increases and even a decrease is observed at a higher MF content, e.g., the LOI at 45 wt % MF content is the lowest among the five samples. The highest LOI with a value of 29.3 is obtained when MF content is 15 wt % revealing that the flame retardance of DMRP greatly depends on the proportion of MF resin and CMRP.

It has been well accepted that there is a nitrogen–phosphorus synergistic behavior in some kinds of flame retardants containing N and P. Generally speaking, the N-P synergism is explained as the interaction between N-containing and P-containing compounds that can produce macromolecular substances such as $(PNO)_X$ or $(PN)_X$ with high thermal stability to consolidate the condensed phase.[25] Accordingly, the combination of RP and MF resin may also have such synergistic effects. However, the conventional way to prepare an N-P synergistic system is by simply mixing the two components and the flame retardance of the system strongly depends on the N/P ratio.[26,27] These research results are fully in agreement with our investigation as the highest LOI is obtained only at 15 wt % MF content level. Besides, in practical applications, it is preferred to conduct a predispersing process rather than mix the two components directly with the matrix resin because a uniform mixing is always difficult to achieve by mechanical mixing. Therefore, we prepared a double-layered microencapsulated synergistic system of RP/ATH/MF, thus simultaneously realized the improvement of the flame retardance and homogeneous dispersion of N-containing and P-containing compounds.

In Figure 7, the LOI values of composites at different FR loading level are compared. Obviously, both of the curves present an increasing trend as FR loading level increases, and the DMRP curve is significantly higher than that of CMRP at each test point. Especially, on addition of 35 wt % DMRP, LOI reaches 31.4 while it is only 27.8 for CMRP sample.

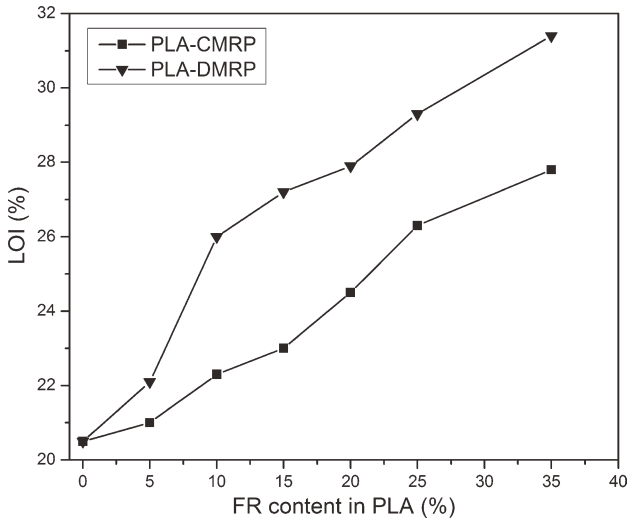

Figure 7 Influence of different FR loading on LOI value (CMRP: RP/ATH = 85%/15%, DMRP: RP/ATH/MF = 72.25%/12.75%/15%).

TABLE II
Results of Combustion Test

Sample	LOI	Dripping	UL 94 rating
PLA	20.5	Y[a]	NC[b]
PLA-RP	27.0	Y	V-2
PLA-CMRP	26.3	Y	V-2
PLA-DMRP	29.3	N[c]	V-0

CMRP: RP/ATH = 85%/15%, DMRP: RP/ATH/MF = 72.25%/12.75%/15%.
[a] Y, having melt dripping.
[b] NC, not classified.
[c] N, having no melt dripping.

It demonstrates that DMRP has superior flame retardance as compared to CMRP. This can be attributed to the N-P synergism and the endothermic decomposition of MF resin, during which water and nitrogen compounds are generated and act as inert gases diluting the oxygen and fuel, thus the thermal stability of the composites is improved. Results of the UL94 test are shown in Table II, each sample with a FR loading of 25 wt %. Plain PLA shows LOI = 20.5, and does not pass the UL94 test. It is highly combustible and burns with flammable melt dripping. The LOI increases to 27.0 when 25 wt % RP was added, and a decrease (only 26.3) occurred after RP was microencapsulated by ATH. Both of the samples presented a short combustion time, but burned with heavy flammable melt dripping in the second flame ignition so as to reach V-2 ranking in the UL94 test. DMRP provides a synergistic effect so that the LOI is increased to 29.3 and it also results in a V-0 rating because only in this formulation no drippings occur. From the photographs of the residue of PLA-DMRP after UL94 test (Fig. 8), it can be seen that the surface of the burned sample is covered with an expanded char network having a lot of holes and fissures. Such characteristics strongly suggest that the char network formed in RP/ATH/MF formulation will protect the surface of the specimen from burning to provide PLA with high flame retardant performance.

However, it is interesting to find that a large amount of white smoke, which could be mainly regarded as oxides of phosphorus, was produced when the PLA-RP sample was burning. But after the incorporation of ATH, e.g., PLA-CMRP or PLA-DMRP, such a phenomenon disappeared. A possible reason is the function of ATH as a smoke suppressant. The heat dissipation by ATH is thought to aid in forming char rather than forming smoke by favoring crosslinking reaction over soot formation, the char provides a fuel-oxygen barrier on the surface of the burning polymer. Besides, ATH will also take part in a chemical reaction with phosphorus at higher temperature. The X-ray diffraction spectrum [Fig. 9(a)] shows clearly that phosphorus oxide (P_2O_5–ICDD n^0 23-1301) and aluminum phosphate ($AlPO_4$–ICDD n^0 11-0500) are produced during the heating process so as to reduce the white smoke. But for PLA-DMRP [Fig. 9(b)], no significant diffraction peaks appear, it exhibits smooth and broad features typical of amorphous structures.

Thermal stability

The TGA curves of plain PLA and the flame-retarded composites both in air flow and nitrogen flow are shown in Figure 10 and the related data are listed in Table III. Here, T_5 (T_{50}) is defined as the temperature when 5% (50%) weight loss occurs and T_{max}, the temperature at maximum weight loss rate. As shown in Figure 10(a), plain PLA starts decomposing at about 340°C (T_5). It also can be seen that the thermal degradation process of PLA includes only one stage of weight loss with a T_{max} of 379°C, and there remains no residue at the end. A first order kinetics analysis gives its activation energy E_A

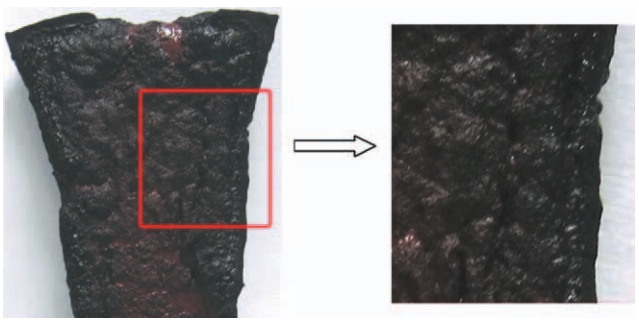

Figure 8 Digital photographs of PLA-DMRP sample after UL94 test (DMRP: RP/ATH/MF = 72.25%/12.75%/15%).[Color figure can be viewed in the online issue, which is available at wileyonlinelibrary.com.]

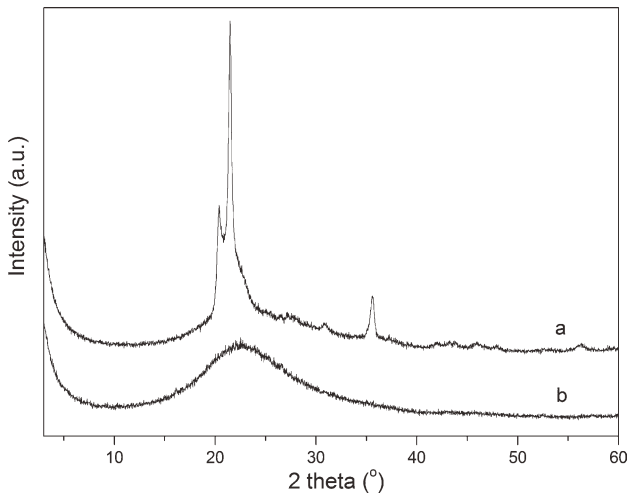

Figure 9 X-ray spectra of (a) PLA-CMRP, (b) PLA-DMRP.

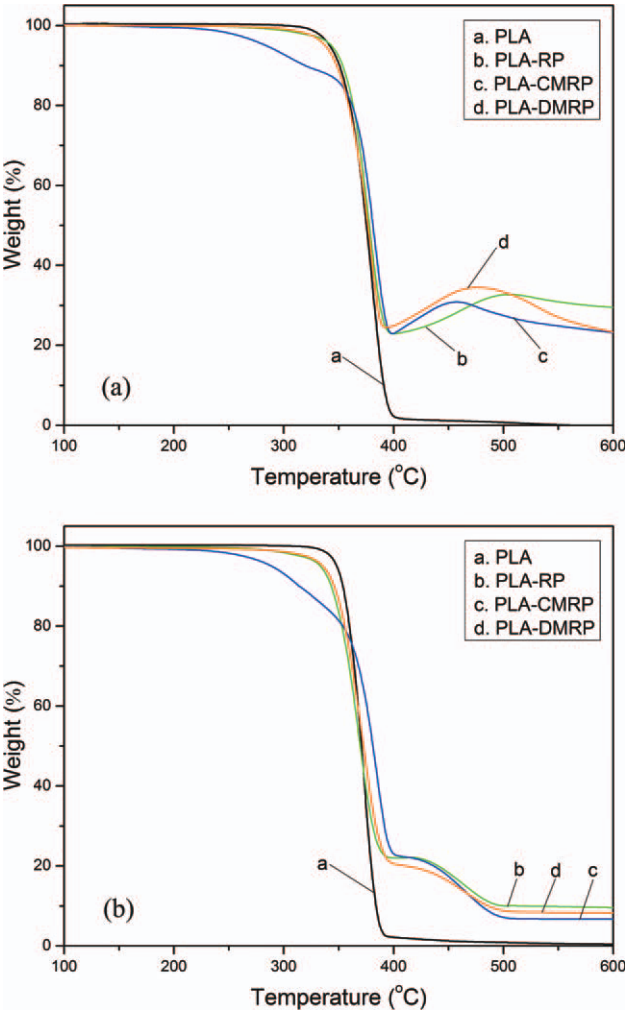

Figure 10 TGA curves of PLA, PLA-RP, PLA-CMRP, and PLA-DMRP with a FR loading of 25 wt % in (a) air flow, (b) nitrogen flow (CMRP: RP/ATH = 85%/15%, DMRP: RP/ATH/MF = 72.25%/12.75%/15%).[Color figure can be viewed in the online issue, which is available at wileyonlinelibrary.com.]

= 261.5 kJ mol^{-1} for the weight loss peak (weight loss 5–95%). The thermal decomposition of PLA is very complicated and much research work has been done about it.[28,29] Generally speaking, based upon a hydroxyl end-initiated ester interchange process giving cyclic oligomers, lactide, acetaldehyde, and carbon monoxide at low temperature, PLA will further degrade by an electron impact-induced mechanism by elimination of the same products and also CO_2 and methylketene as well as other fragments at higher temperature.

However, the addition of flame retardants changes its decomposition pattern. The PLA-RP [Fig. 10(a)] has a TGA curves similar to that of PLA at low temperature with a slight shift to the right when above 340°C and its T_5, T_{50}, and T_{max} almost remain the same, indicating that RP has certain flame retardance in PLA. The flame retardance mechanisms of RP could be described as two processes involving condensed phase and gas phase. At the beginning, RP undergoes an oxidation process, and its resultants, mainly P_4O_6 and P_4O_{10}, will then react with water vapor generated from the polymer matrix. The following oxyacid of phosphorus will first cover the surface of the burning substrate and further promote the dehydration of polymers to form a protective char layer. While in gas phase, phosphorus-containing compounds have been reported to scavenge carrier species such as H· and HO· radicals in burning process that are required during the oxidation of volatile pyrolytic products in the flame.[15,30] However, there is a weight increment in the range of 400–505°C along with greatly increased residue at 600°C. But it disappears in Figure 10(b), thus we can conclude that the weight increment arises from a series of reactions of RP as explained above. For PLA-CMRP [Fig. 10(a)], it can be found in Table III that CMRP lowers the temperature of T_5 by 54°C, but increases T_{50} and T_{max} by 6 and 4°C as compared to that of plain PLA, respectively. The weight loss observed is developed within a wider temperature range than that of plain PLA and PLA-RP. Derivative of its TGA curve shows three temperature peaks. The lower temperature peak is well defined at 307°C representing the severe decomposition of ATH. The second temperature peak is at about 382°C, while the third peak is at 473°C corresponding to a wide zone not well defined. A possible reason for this is the dehydration of oxyacid of phosphorus and the chemical reaction between phosphorus and aluminum at higher temperature as confirmed by XRD.

The onset temperature 338°C, T_5 of PLA-DMRP [Fig. 10(a)], is slightly lower than that of plain PLA and PLA-RP and much higher than that of PLA-

TABLE III
TGA Data of All Samples in Air Flow

Sample	T_5 (°C)	T_{50} (°C)	T_{max} (°C)	Residue (%)		
				400°C	500°C	600°C
PLA	342	375	379	2.32	0.73	0
PLA-RP	343	378	377	22.89	32.63	29.49
PLA-CMRP	284	381	383	22.96	27.47	23.19
PLA-DMRP	338	377	379	24.88	33.35	23.34

CMRP due to the relatively low decomposition temperature of MF resin as well as encapsulation of ATH. Moore et al.[31] reported that the thermal degradation of MF resin involved methylene and/or methylene ether bridges and possibly methylol groups in air below about 250°C, and breakdown of these groups and loss of melamine would occur above 250°C. Melamine decomposes at 300–395°C, and large quantities of nonflammable gases such as NH_3 and CO_2 are then released, which are helpful in forming a "honeycomb" char structure. Moreover, due to the consolidation effect of N-P synergism, a more stable and compact char layer will be formed, thus the release of the pyrolytic products are effectively controlled and its weight loss rate becomes lower than the others resulting in an increased residue of 24.88 and 33.35%, at 400 and 500°C respectively.

CONCLUSIONS

A novel double-layered microencapsulated RP was successfully prepared through chemical precipitation of aluminum trihydrate and *in situ* polymerization of melamine formaldehyde resin. The encapsulated product shows a higher ignition point as well as lower moisture absorption rate as compared to that of plain RP, which indicates that a pyknotic encapsulation is formed as it also can be seen in SEM images. With an optimum mass ratio of RP/ATH/MF = 72.25%/12.75%/15%, the incorporation of DMRP in PLA has greatly improved the flame retardance and thermal stability of PLA. The LOI value of the binary composites increases gradually with the increase of DMRP content and the V-0 rating is achieved at 25 wt % loading level, while digital photographs confirm that the PLA composites can form a dense intumescent char network with a certain degree of expansion. As a distinct synergistic N-P system, DMRP gives full play to its flame retardation in condensed phase and gas phase including surface protection by phosphorus-containing acid catalysis of char formation, heat dissipation by ATH as well as N-P synergism.

References

1. Yu, L.; Dean, K.; Li, L. Prog Polym Sci 2006, 31, 576.
2. Tsuji, H.; Sumida, K. J Appl Polym Sci 2001, 79, 1582.
3. Ouchi, T.; Ohya, Y. J Polym Sci Part A: Polym Chem 2004, 42, 453.
4. Heiss, C.; Kraus, R.; Peters, F.; Henn, W.; Schnabelrauch, M.; Berg, A.; Pautzsch, T.; Weisser, J.; Schnettler, R. J Biomed Mater Res B Appl Biomater 2009, 90B, 55.
5. Takei, T.; Yoshida, M.; Hatate, Y.; Shiomori, K.; Kiyoyama, S.; Tsutsui, T.; Mizuta, K. J Appl Polym Sci 2008, 109, 763.
6. Auras, R.; Harte, B.; Selke, S. Macromol Biosci 2004, 4, 835.
7. Plackett, D. V.; Holm, V. K.; Johansen, P.; Ndoni, S.; Nielsen, P. V.; Malm, T. S.; Södergård, A.; Verstichel, S. Packag Technol Sci 2006, 19, 1.
8. Serizawa, S.; Inoue, K.; Iji, M. J Appl Polym Sci 2006, 100, 618.
9. Vink, E. T. H.; Rábago, K. R.; Glassner, D. A.; Gruber, P. R. Polym Degrad Stab 2005, 80, 403.
10. Meinander, K.; Niemi, M.; Hakola, J. S.; Selin, J.-F. Macromol Symp 1997, 123, 147.
11. Fontaine, G.; Bourbigot, S. J Appl Polym Sci 2009, 113, 3860.
12. Ni, J.; Song, L.; Hu, Y.; Zhang, P.; Xing, W. Polym Adv Technol 2009, 20, 999.
13. Zhan, J.; Song, L.; Nie, S.; Hu, Y. Polym Degrad Stab 2009, 94, 291.
14. Yamashita, T.; Mizuno, K.; Ueno, T.; Ishikawa, T. Kobunshi Ronbunshu 2008, 65, 288.
15. Wu, Q.; Lü, J.; Qu, B. Polym Int 2003, 52, 1326.
16. Bonin, Y.; LeBlanc, J. US Patent 4,985,485, 1989.
17. Li, S.; Yuan, H.; Yu, T.; Ren, J. Polym Adv Technol 2009, 20, 1114.
18. Ren, J.; Liu, Z. C.; Ren, T. Polym Polym Compos 2007, 15, 633.
19. Li, S.; Ren, J.; Yuan, H.; Yu, T.; Yuan, W. Polym Int 2010, 59, 242.
20. Laoutid, F.; Ferry, L.; Cuesta, J. M. L.; Crespy, A. Polym Degrad Stab 2003, 82, 357.
21. Haurie, L.; Fernández, A. I.; Velasco, J. I.; Chimenos, J. M.; Cuesta, J.-M. L.; Espiell, F. Polym Degrad Stab 2006, 91, 989.
22. Kopinke, F.-D.; Remmler, M.; Mackenzie, K.; Möder, M.; Wachsen, O. Polym Degrad Stab 1996, 53, 329.
23. Wu, K.; Wang, Z.; Liang, H. Polym Compos 2008, 29, 854.
24. Huang, H.; Tian, M.; Liu, L.; Liang, W.; Zhang, L. J Appl Polym Sci 2006, 100, 4461.
25. Costa, L.; Camino, G. ACS Symposium Series 425, Washington DC 1990.
26. Xiao, J.; Hu, Y.; Yang, L.; Cai, Y.; Song, L.; Chen, Z.; Fan, W. Polym Degrad Stab 2006, 91, 2093.
27. Gaan, S.; Sun, G.; Hutches, K.; Engelhard, M. H. Polym Degrad Stab 2008, 93, 99.
28. Kricheldorf, H. R.; Lüderwald, I. Die Makromol Chem 1978, 179, 421.
29. Jacobi, E.; Lüderwald, I.; Schulz, R. C. Die Makromol Chem 1978, 179, 429.
30. Smith, C. S.; Metcalfe, E. Polym Int 2000, 49, 1169.
31. Moore, W. R.; Donnelly, E. J Appl Chem 1963, 13, 537.